Artificial Intelligence and Computational Methods in Applied Science,
AICOMAS 2025
February 17-21, 2025, Paris, France

Modeling of Highly Porous Materials under Extreme Loading using Deep Learning

M. Giselle Fernández-Godino, Meir H. Shachar, Kevin A. Korner, William J. Schill, Charles F. Jekel, Jonathan L. Belof

Lawrence Livermore National Laboratory

LLNL-CONF-2002671
This work was performed under the auspices of the U.S. Department of Energy by Lawrence Livermore National Laboratory under contract DE-AC52-07NA27344. Lawrence Livermore National Security, LLC

Lawrence Livermore National Laboratory

SLIDE ORGANIZATION

Comprehensive Title

CONTENT

Takeaway message

MOTIVATION

Accelerating Scientific Discovery and Predict Physics Without Full-Scale Computation

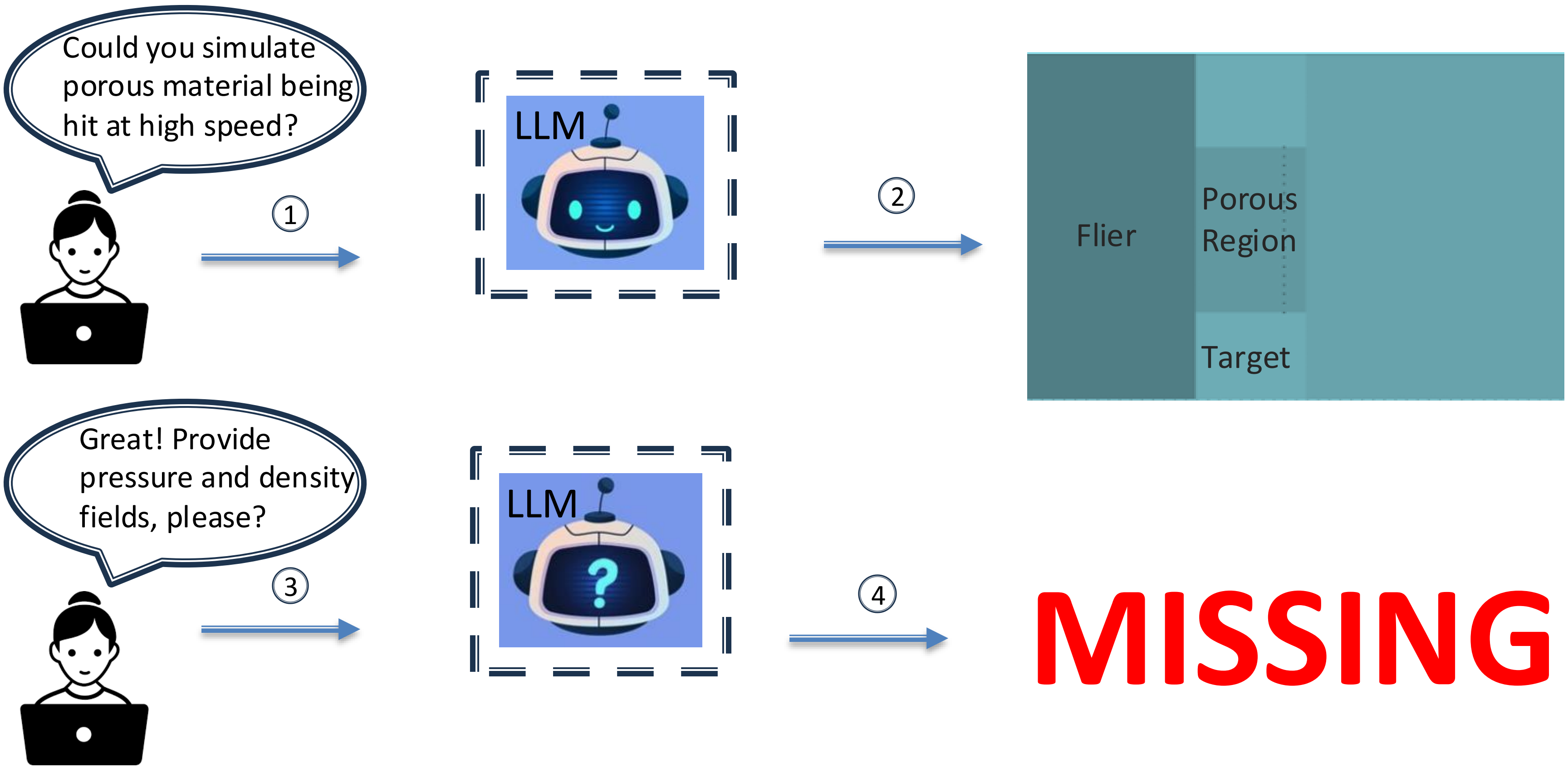

Large Language Models (LLMs) **understand and generate text/**videos. Can we build similar models for **simulating physics**?

Predicting Temporal Evolution through Physics Simulations is Computationally Expensive

Challenge:

- High-fidelity simulations require **expensive iterative solvers**.
- Model reduction techniques often **lose key dynamics**.

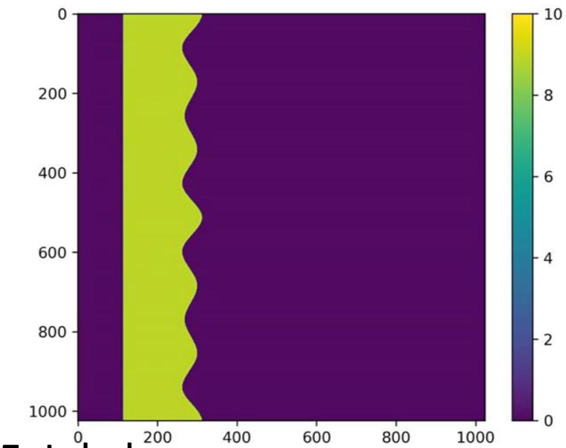

C. F. Jekel

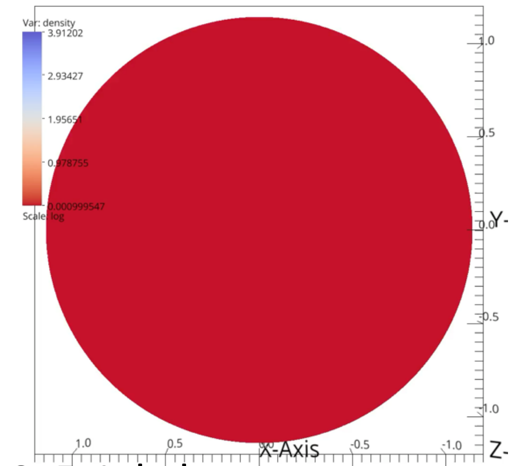

C. F. Jekel

Goal:
Develop an **ML model** that learns spatio-temporal fields evolution from simulation data, reducing computational cost.

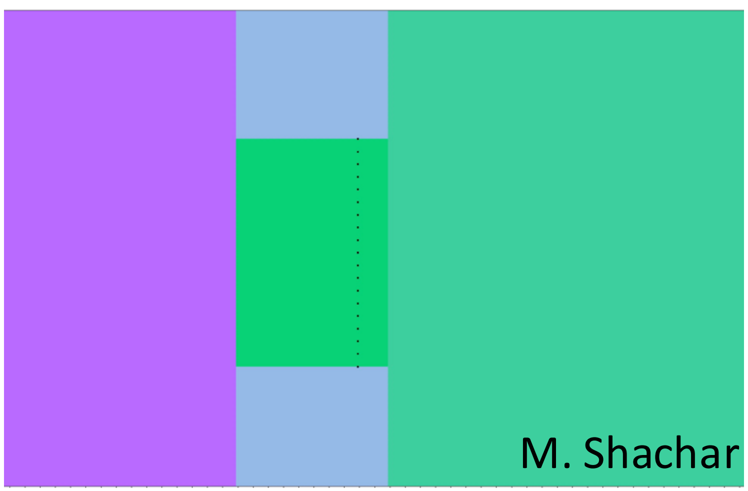

M. Shachar

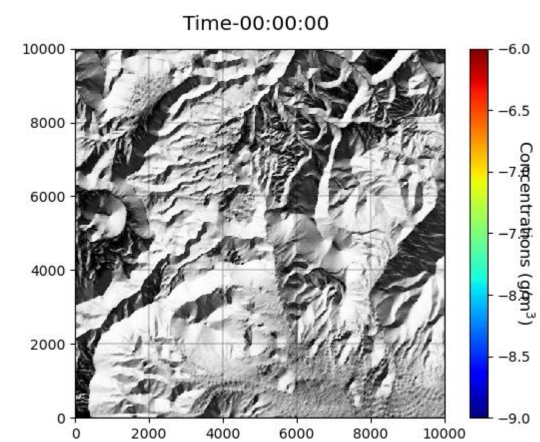

M. G. Fernández-Godino

We can train **LLMs to run physics** simulations. Physics simulations are **expensive,** can we accelerate the process training LLMs using **ML models**?

SIMULATION DATA

The Problem of Interest is a Highly Porous Material under Extreme Loading

Porous materials exhibit complex shock responses:

- **Anomalous responses** where higher pressure behind the shock front leads to lower density.
- Significantly **reduced shock wave speeds** compared to fully dense materials, varying smoothly with porosity.

Controlling porosity distributions can achieve **variable shock speeds**, allowing for **precise wave shape control**, **management of interfacial instabilities** and **energy** (Jones et al., 2018; Huy Pham et al., 2023).

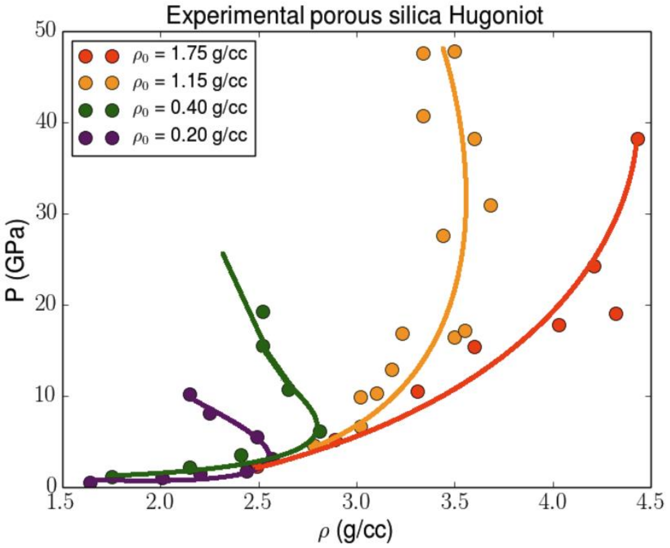

Trunin et al., 2001

Goal: Simulations are expensive. Develop a **neural network-based ML model** that learns spatio-temporal evolution from simulation data, reducing computational cost.

Many Hydrodynamic Simulations Were Ran to Obtain Enough Data for ML Training

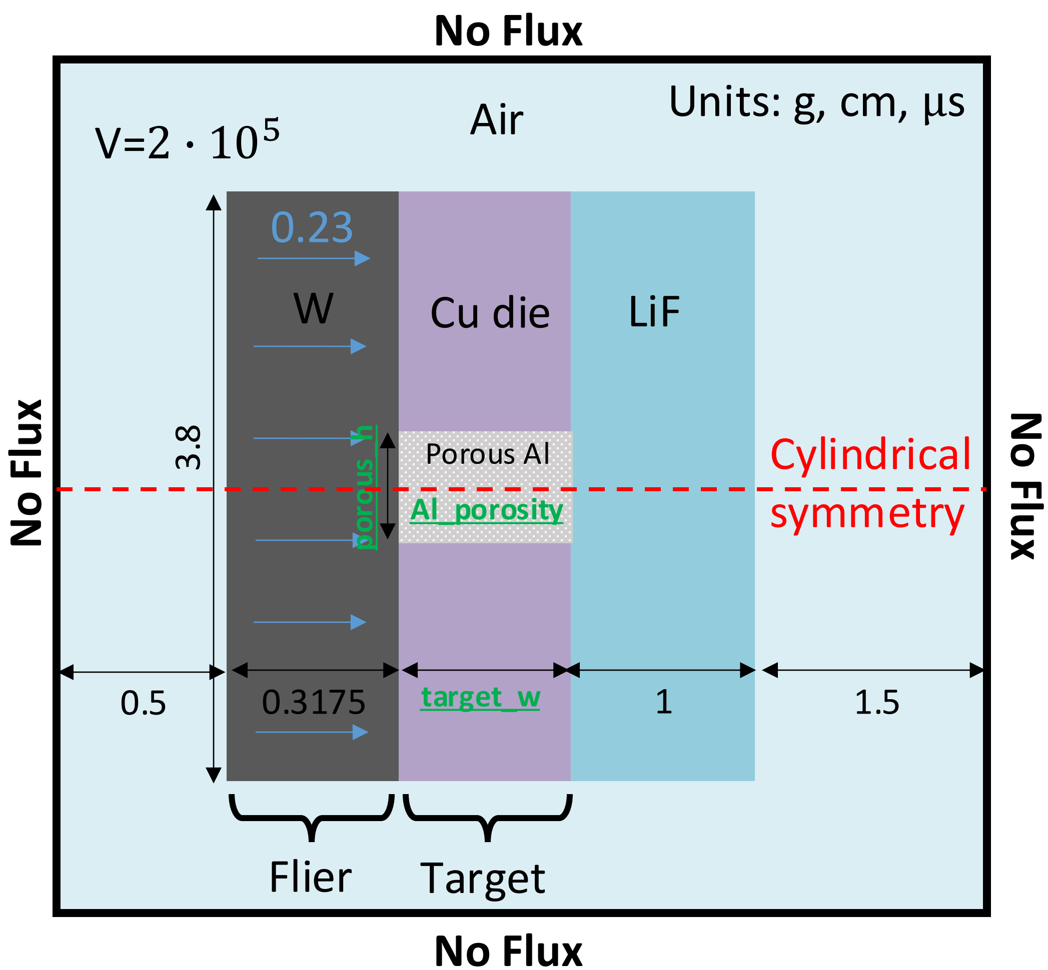

Hydrocode: **Marbl**

Number of time-steps per simulations: **61 (~12μs)**

Number of fields:**7**

Spatial resolution: **60x60**

Studied variables:
0.2 cm < **target_w** < 1.0 cm
0.05 cm < **porous_h** < 3.8 cm
0.05 < **Al_porosity** < 0.75

Number of simulations:**1000**
Sampling technique = **Latin Hypercube Sampling**

Training ML models for full field temporal simulation predictions require lots of data. Marbl hydrocode was used for this purpose and the geometry specifications are shown above.

Many Hydrodynamic Simulations Were Ran to Obtain Enough Data for ML Training

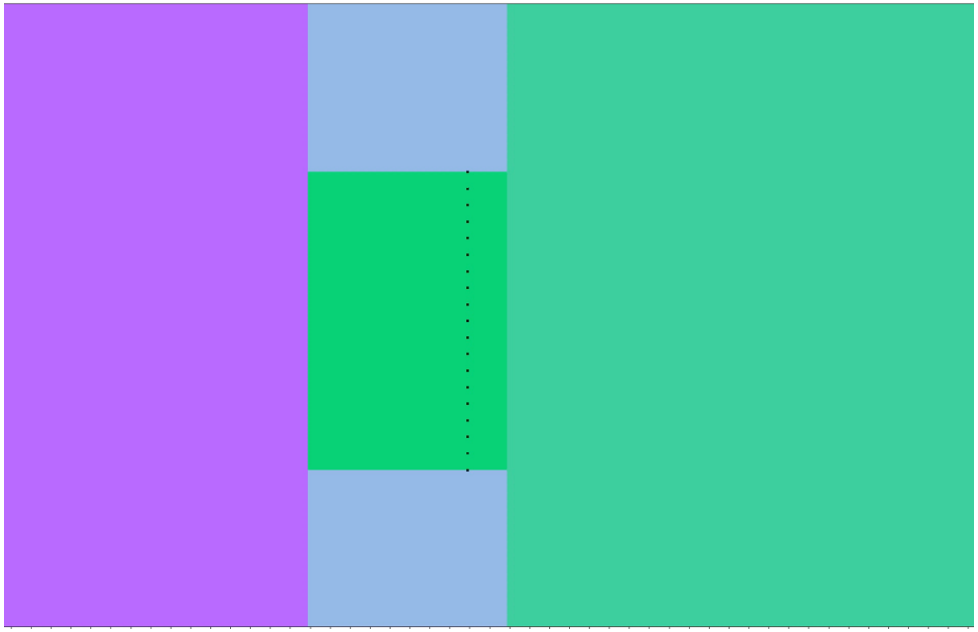

Hydrocode: **Marbl**

Number of time-steps per simulations: **61 (~12μs)**

Number of fields:**7**

Spatial resolution: **60x60**

Studied variables:
0.2 cm < **target_w** < 1.0 cm
0.05 cm < **porous_h** < 3.8 cm
0.05 < **Al_porosity** < 0.75

Number of simulations:**1000**
Sampling technique = **Latin Hypercube Sampling**

Training ML models for full field temporal simulation predictions require lots of data. Marbl hydrocode was used for this purpose and the geometry specifications are shown above.

MACHINE LEARNING MODEL

The ML Model (7STM) Predicts the Shocked Plate Evolution Considering Seven Fields

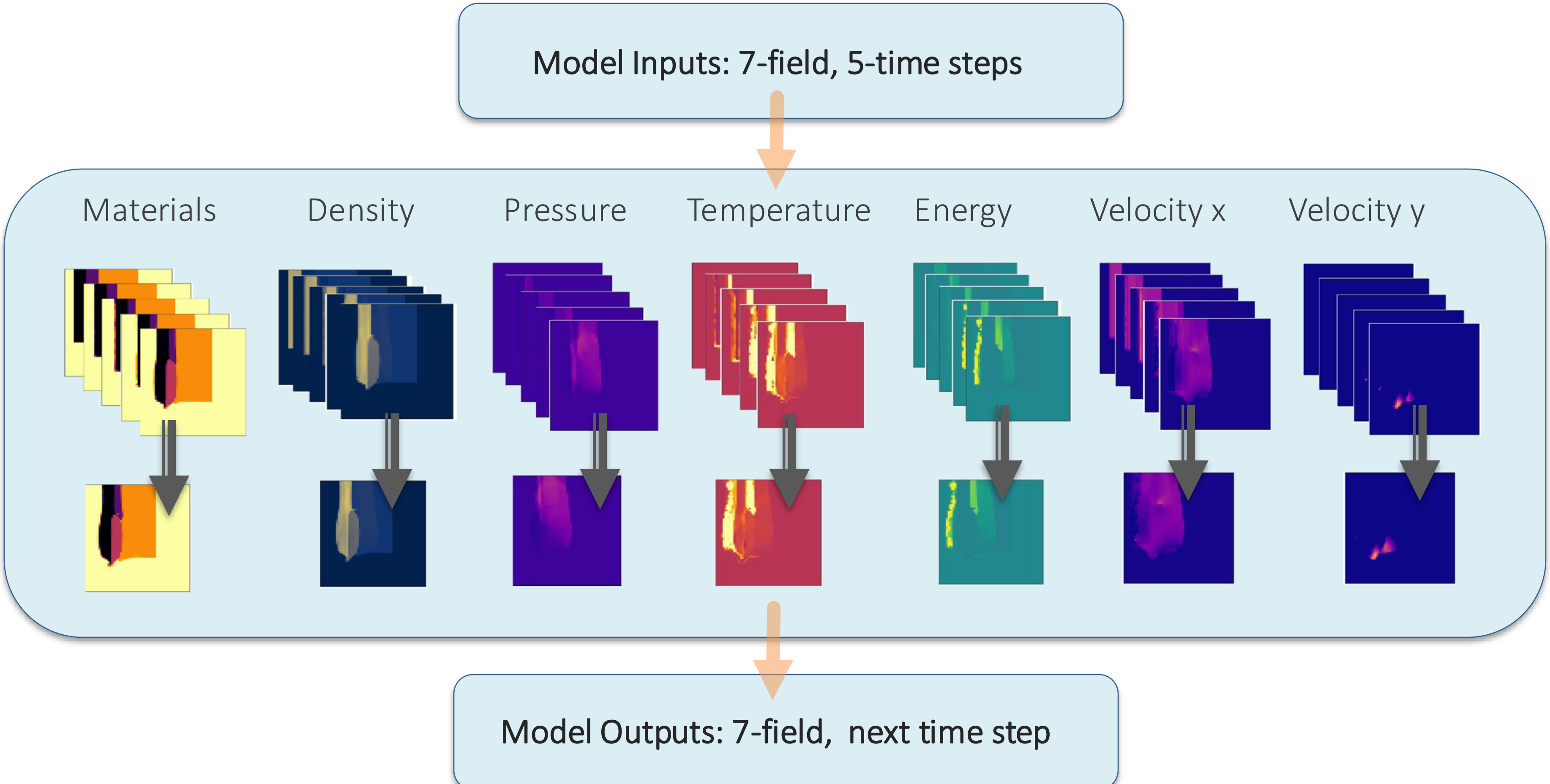

All field values normalized between 0 and 1

7STM receives information of previous steps and is able to predict the following time step for fields Materials, Density, Pressure, Temperature, Energy, Velocity x, and Velocity y.

7STM Receives Five Time Steps and Return the Next Frame.

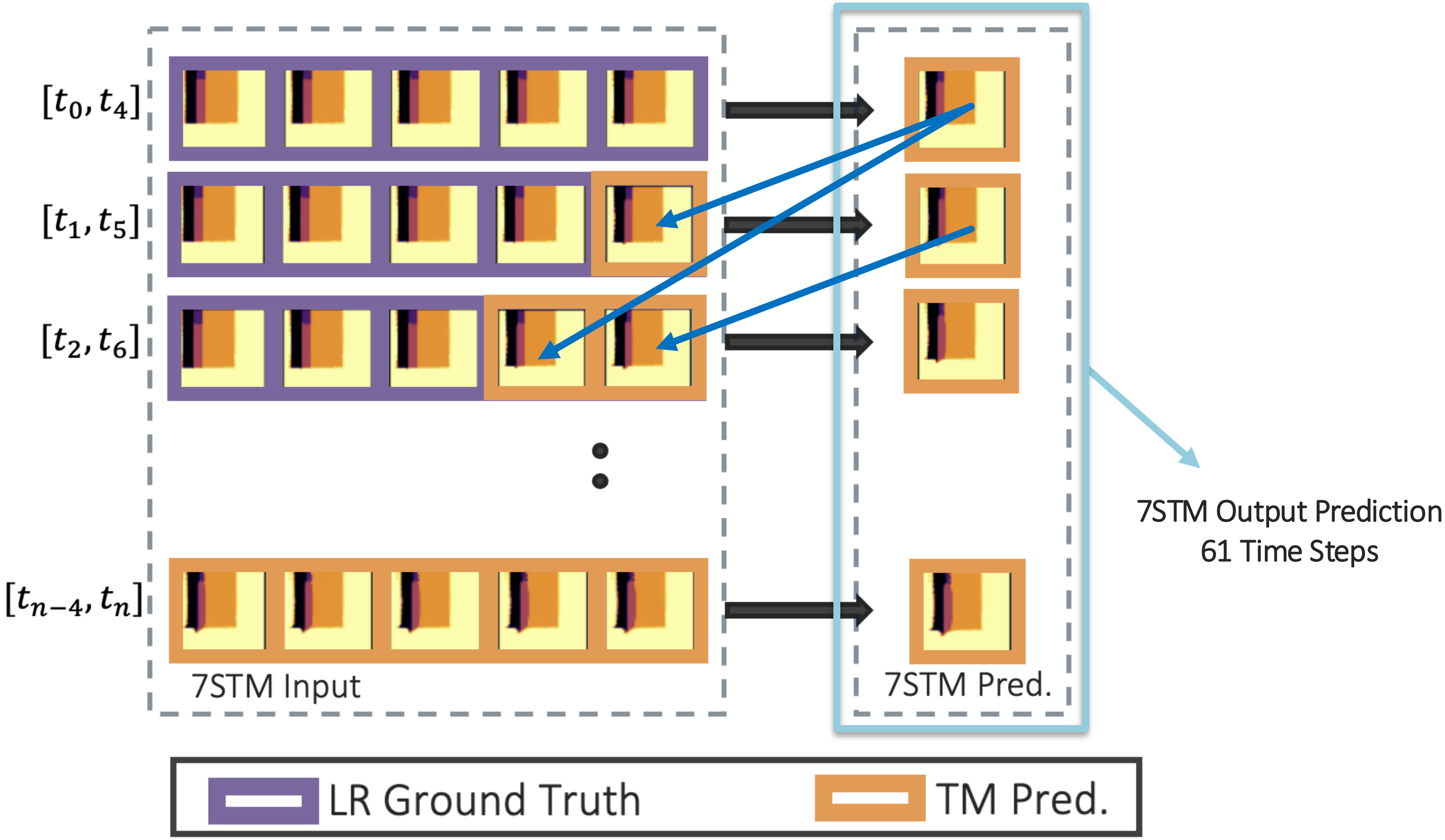

7STM receives fields of previous steps and predict the following time step auto-regressively. The predicted time step is now fed into the input set for the next prediction.

Temporal Autoencoder is the Architecture Used to Predict the 2D Evolution of 7 Fields

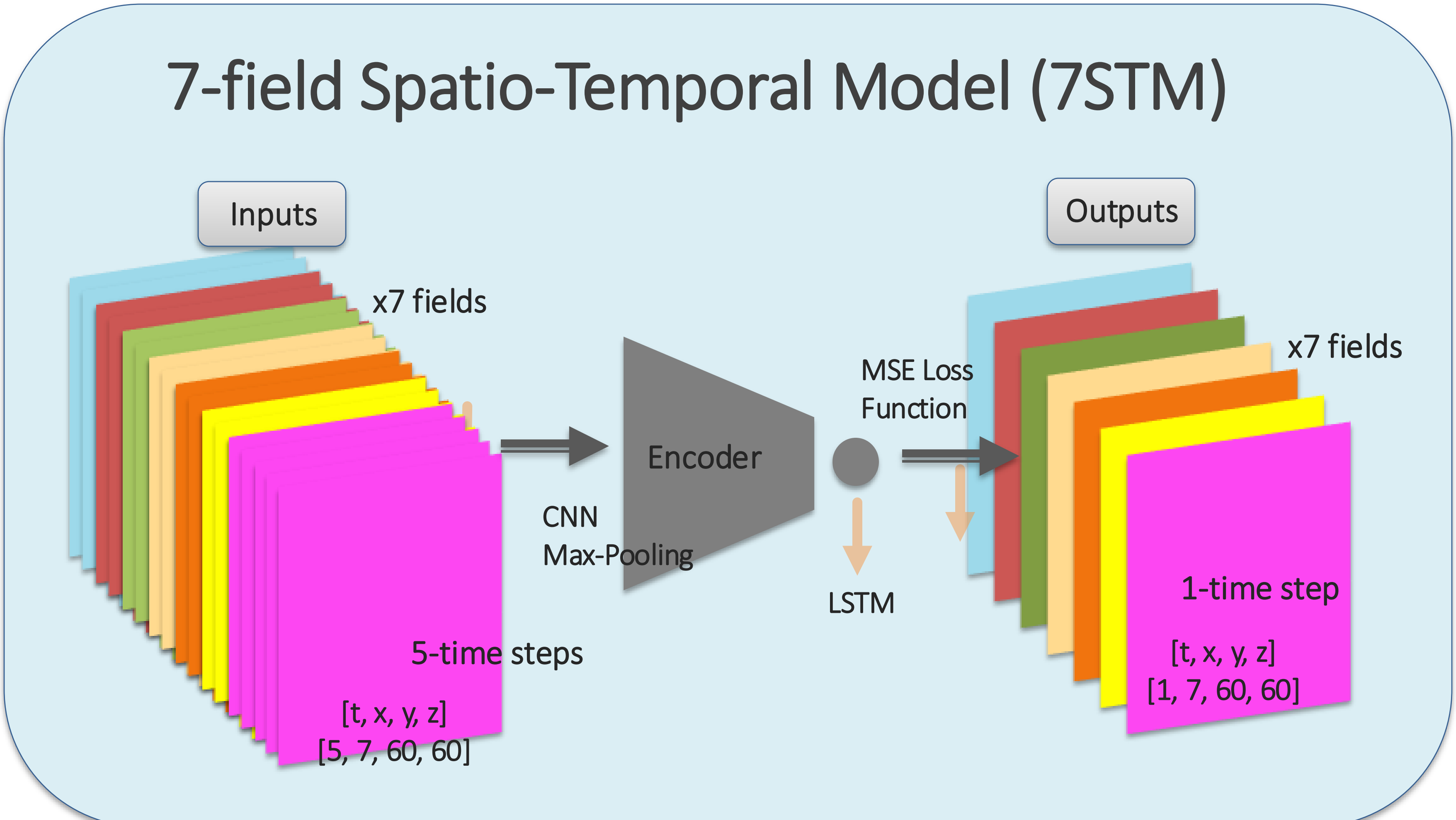

7STM predicts the next time step using a temporal autoencoder with **CNN** and **LSTM**, capturing **spatio-temporal** evolution across **seven fields**.

QUALITATIVE PERFORMANCE

*Field values normalized between zero and one.

Qualitative Performance: Density

*Field values normalized between zero and one.

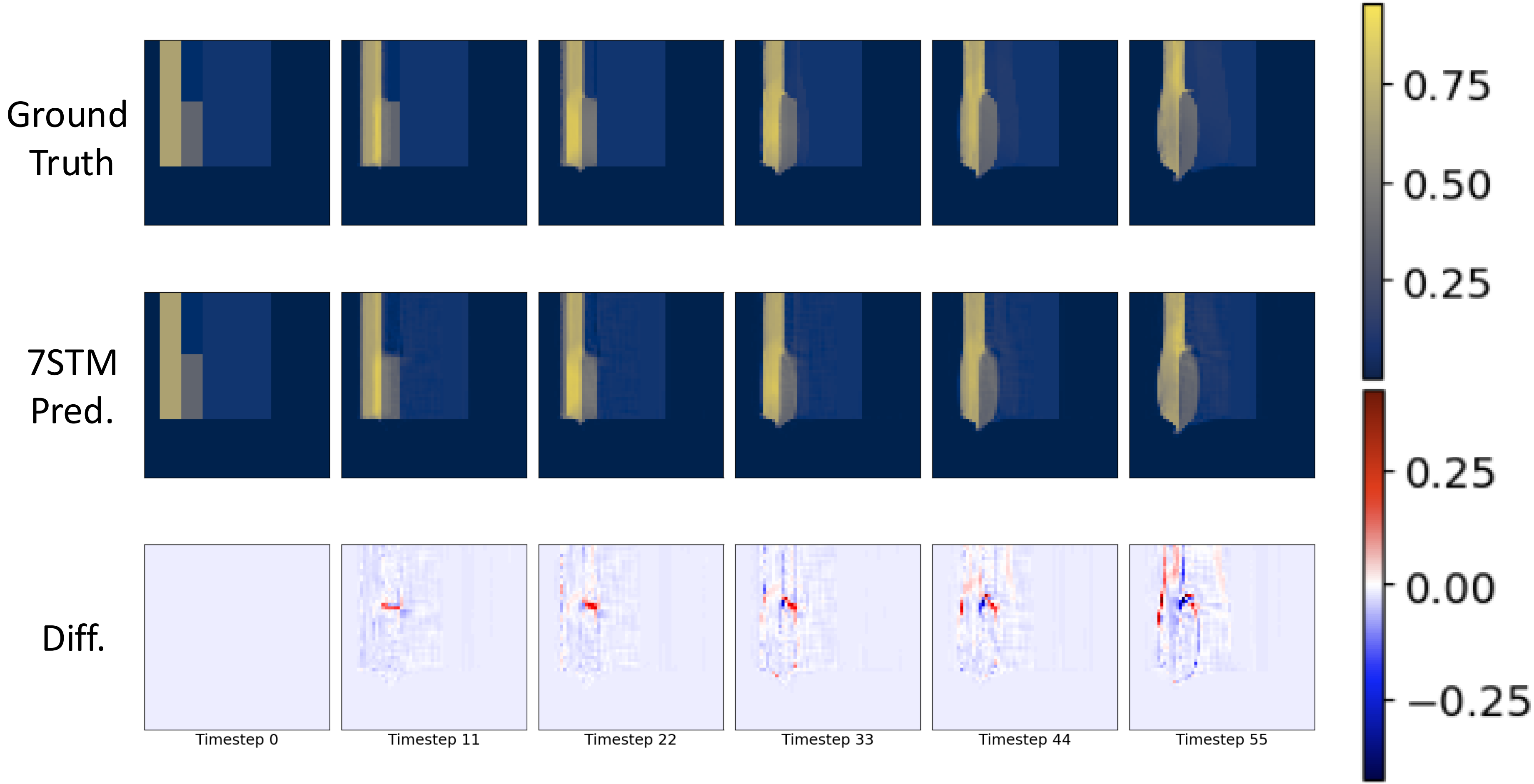

First row is the test sequence (unseen during training), called ground truth (GT); the **second row** is the 7STM prediction, and the **third** shows the difference between GT and 7STM predictions.

Qualitative Performance: Energy

*Field values normalized between zero and one.

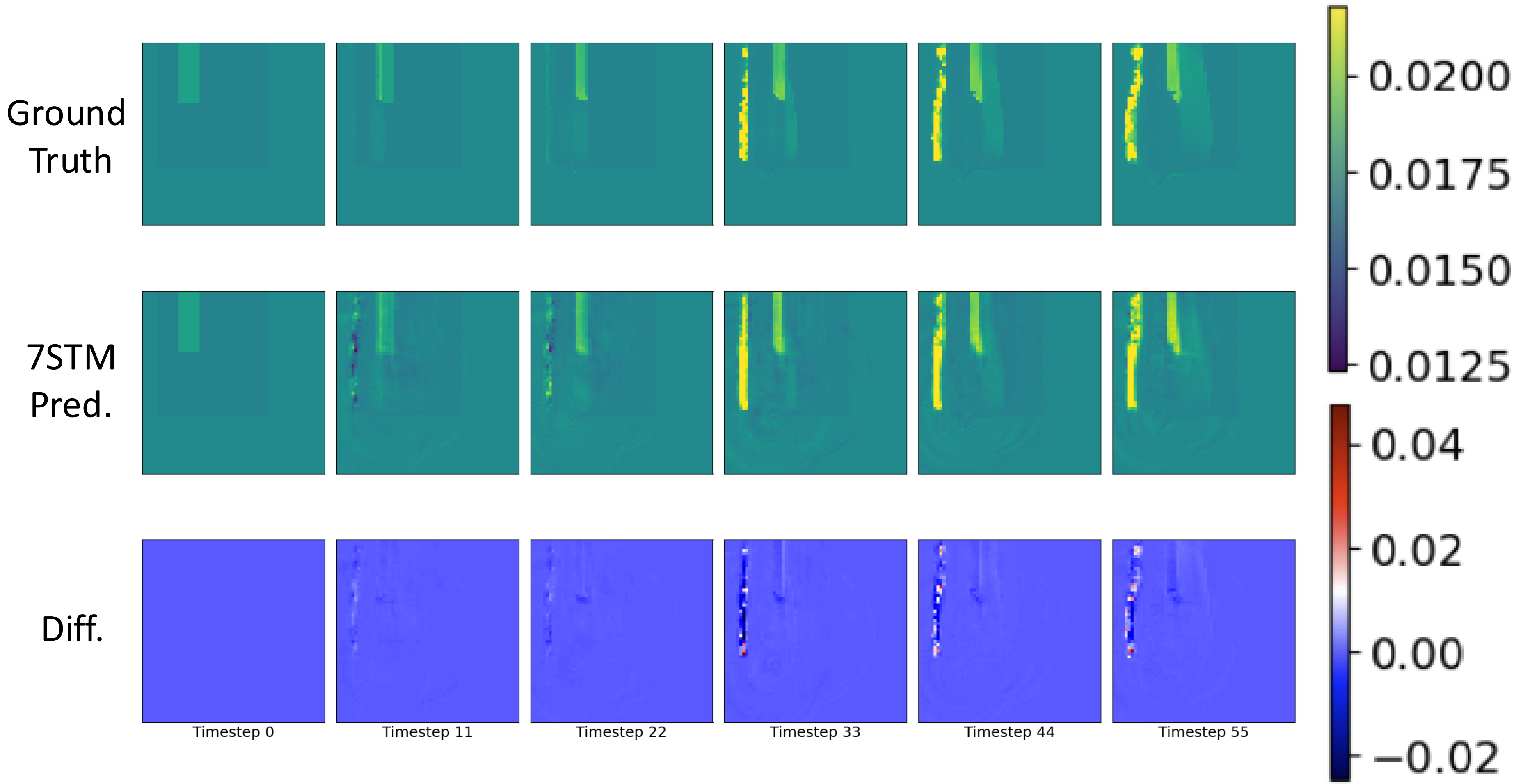

First row is the test sequence (unseen during training), called ground truth (GT); the **second row** is the 7STM prediction, and the **third** shows the difference between GT and 7STM predictions.

Qualitative Performance: Temperature

*Field values normalized between zero and one.

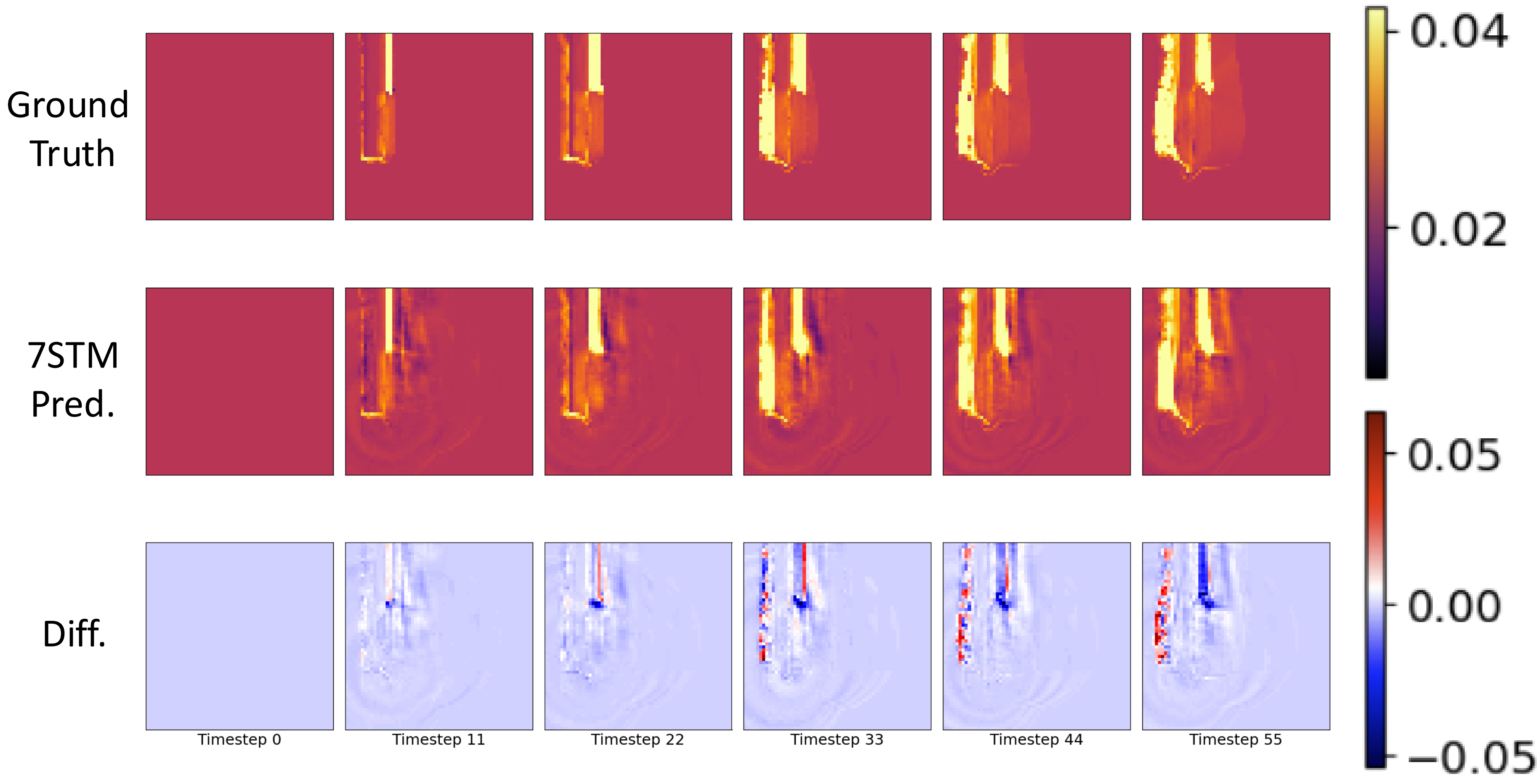

First row is the test sequence (unseen during training), called ground truth (GT); the **second row** is the 7STM prediction, and the **third** shows the difference between GT and 7STM predictions.

Qualitative Performance: Materials

*Field values normalized between zero and one.

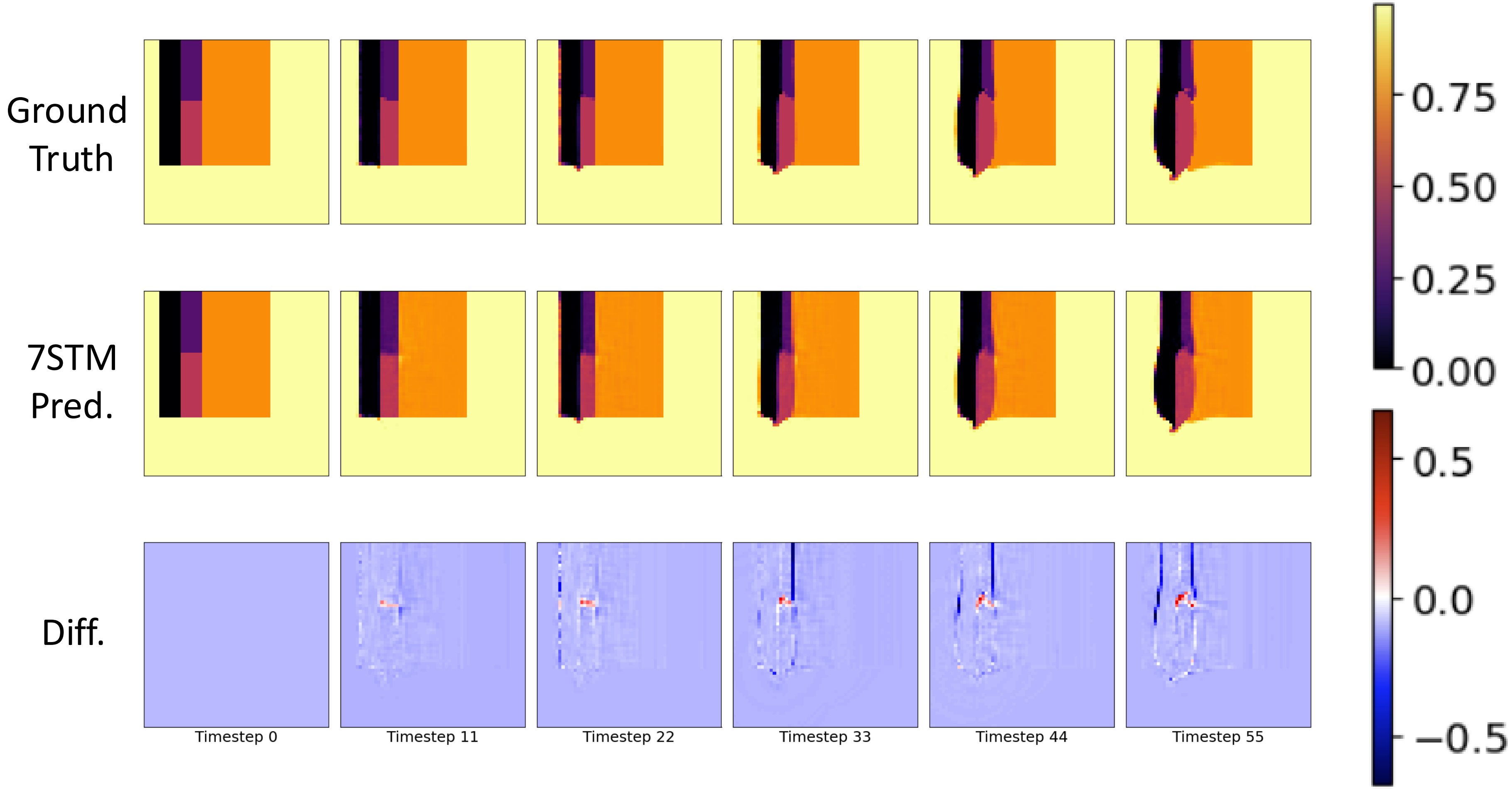

First row is the test sequence (unseen during training), called ground truth (GT); the **second row** is the 7STM prediction, and the **third** shows the difference between GT and 7STM predictions.

Qualitative Performance: Velocity_x

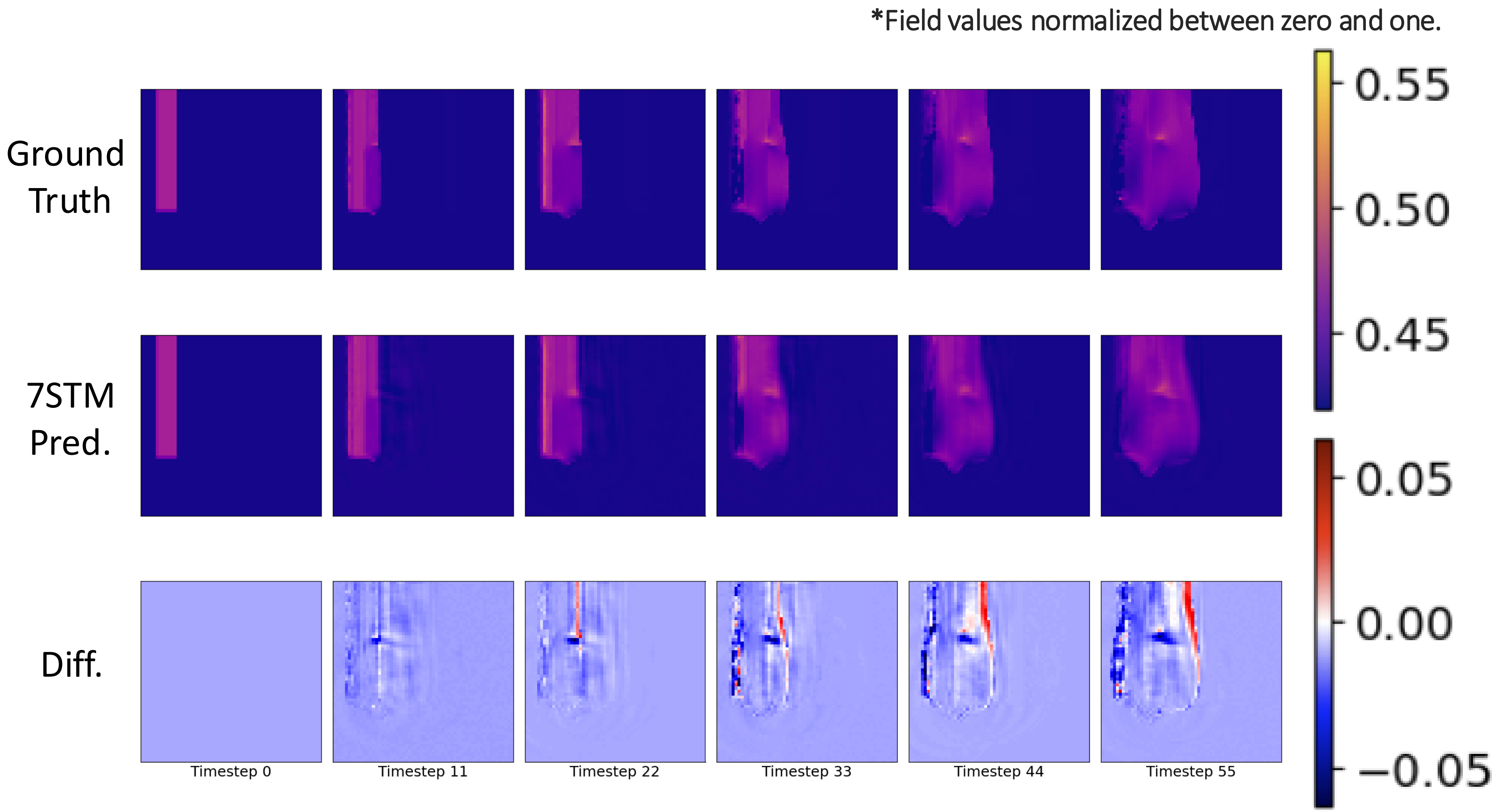

First row is the test sequence (unseen during training), called ground truth (GT); the **second row** is the 7STM prediction, and the **third** shows the difference between GT and 7STM predictions.

Qualitative Performance: Velocity_y

*Field values normalized between zero and one.

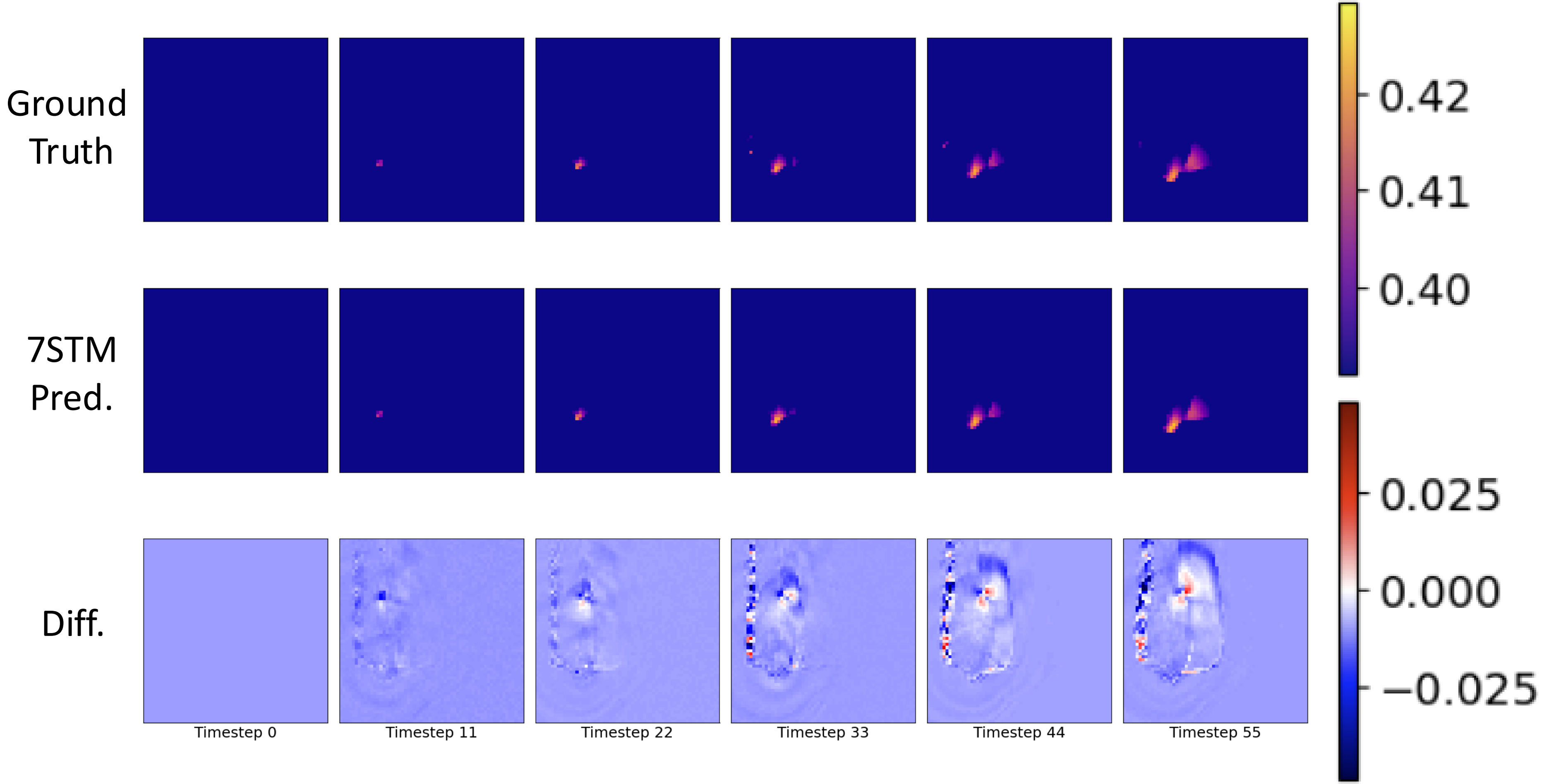

First row is the test sequence (unseen during training), called ground truth (GT); the **second row** is the 7STM prediction, and the **third** shows the difference between GT and 7STM predictions.

Qualitative Performance: Pressure

*Field values normalized between zero and one.

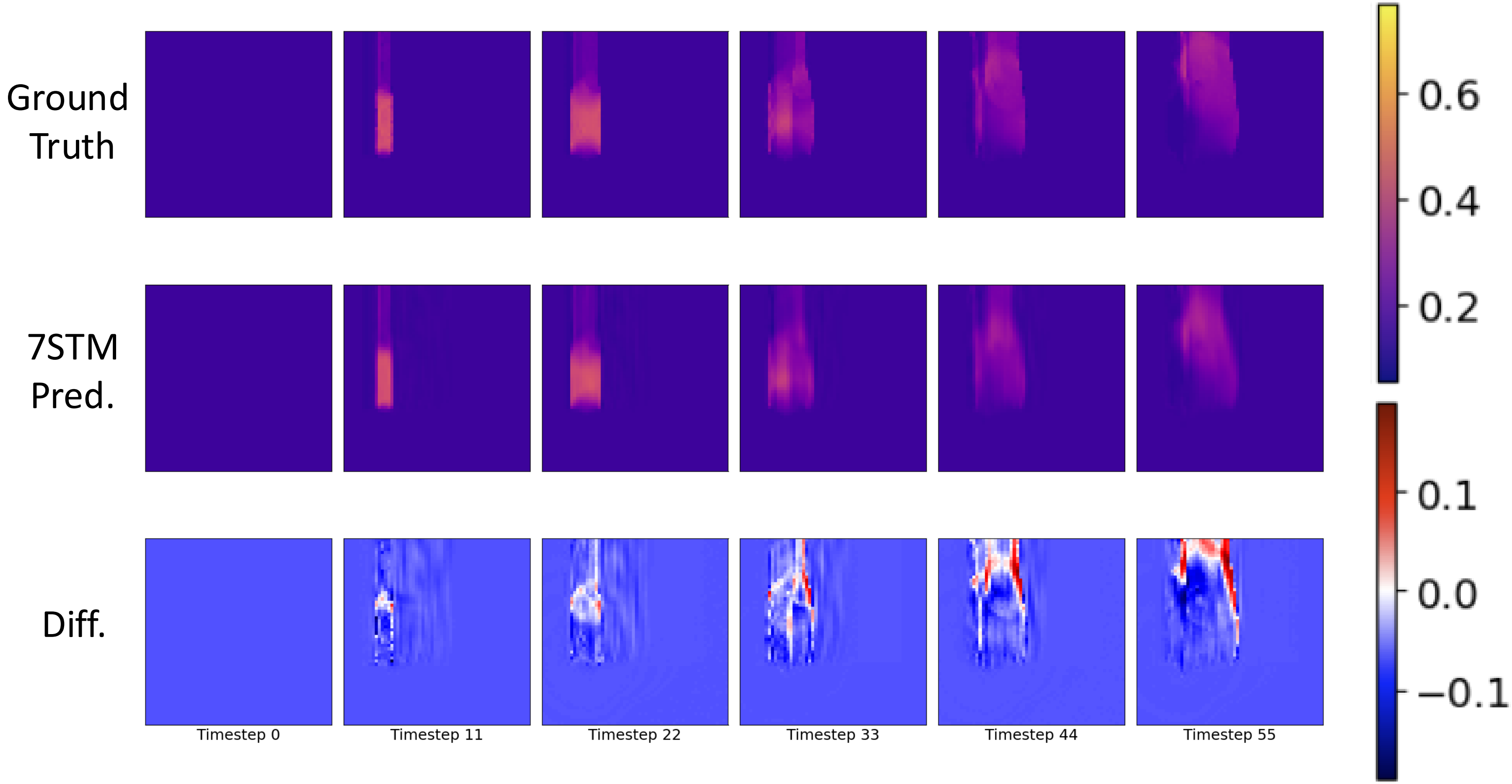

First row is the test sequence (unseen during training), called ground truth (GT); the **second row** is the 7STM prediction, and the **third** shows the difference between GT and 7STM predictions.

QUANTITATIVE PERFORMANCE

7STM's Quantitative Performance on Training and Validation Data as a Function of Epoch

- Trained for 1000 epochs
- Error stabilizes after 1000 epochs
- Smooth error reduction observed in both training and validation datasets
- Validation loss function (MSE) reaches **6e-5**.
- In relative terms MSE represents a **0.005% validation** error.

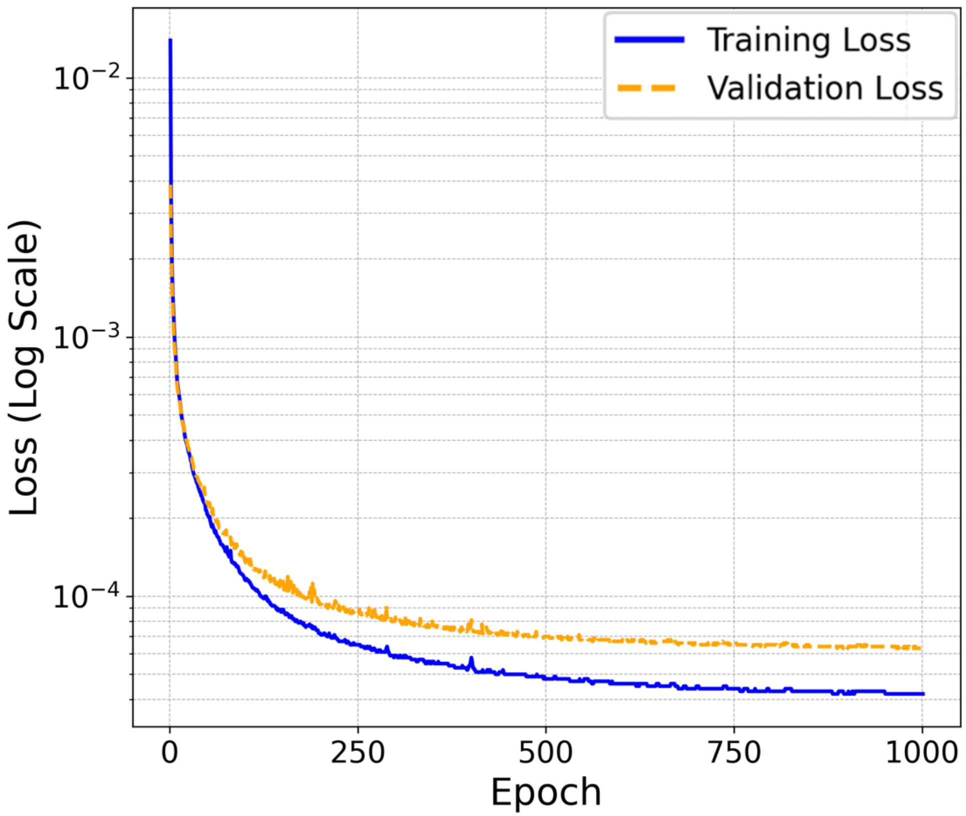

This slide presents the quantitative **performance** of 7STM over the course of **training**, focusing on loss convergence.

Description of the Metrics Used to Assess 7STM's Quantitative Performance

$$\boxed{\text{MSE}} = \frac{1}{N}\sum_{i=1}^{N}(y_i - \hat{y}_i)^2$$

Absolute/Pointwise Error

Where:

- y_i = True value
- $\hat{y}_i$ = Predicted value
- N = Total number of samples

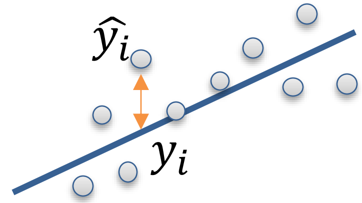

$$\boxed{\text{Conservation of Mass}} = \frac{|M_{\text{pred}} - M_{\text{true}}|}{M_{\text{true}}}$$

Absolute/Pointwise Error

Where:

- M_{pred} = Total mass of the predicted values
- M_{true} = Total mass of the true values

$$\left.\begin{array}{l} M_{true} = 1 \\ M_{pred} = 0.9 \end{array}\right\} \begin{array}{l}\text{Cons.} \\ \text{Mass} = 0.1\end{array}$$

$$\boxed{\text{SSIM}(x, y)} = \frac{(2\mu_x\mu_y + C_1)(2\sigma_{xy} + C_2)}{(\mu_x^2 + \mu_y^2 + C_1)(\sigma_x^2 + \sigma_y^2 + C_2)}$$

Structural/Perceptual Error

Where:

- μ_x and μ_y are the means of x and y
- σ_x^2 and σ_y^2 are the variances of x and y
- σ_{xy} is the covariance between x and y
- C_1 and C_2 are constants to stabilize the division

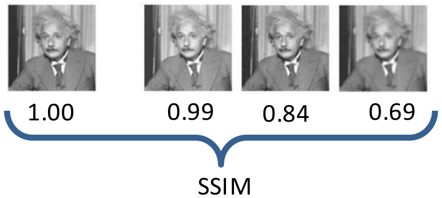

$$\boxed{\text{IoU}} = \frac{|\text{Prediction} \cap \text{Ground Truth}|}{|\text{Prediction} \cup \text{Ground Truth}|}$$

Structural/Perceptual Error

Where:

- $\cap$ represents the intersection (common elements in both sets)
- $\cup$ represents the union (all unique elements in both sets)

For threshold-based binarization:

$$\hat{y}_i = \begin{cases} 1 & \text{if } y_i < \text{threshold} \\ 0 & \text{otherwise} \end{cases}$$

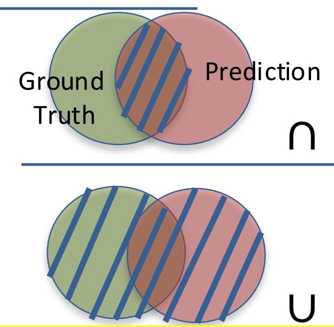

MSE and **Conservation of Mass** assess prediction magnitude accuracy, while **SSIM** and **IoU** evaluate perceptual and structural differences.

7STM's Performance on 91 Test Data Sequences as a Function of Time Step

- The **solid line** represents the **mean** performance across 91 test simulations.
- The **shaded region** denotes **±1 standard deviation** from the mean.
- The **dashed line** indicates the **maximum error** within the trained range.

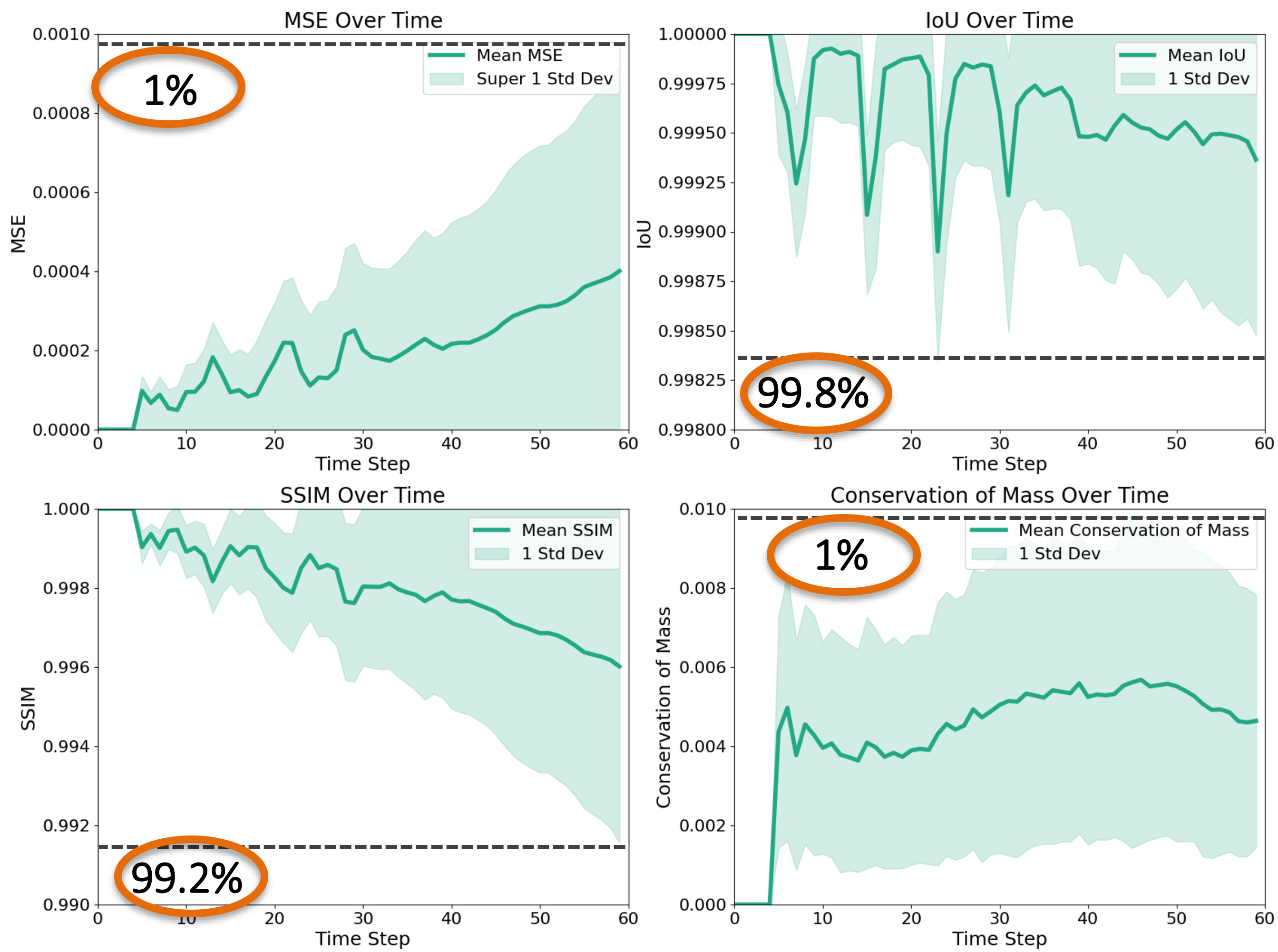

The model demonstrates **exceptional** performance, with **errors consistently below 1%** throughout the simulated/trained time.

7STM's Averaged Performance on 91 Test Data Sequences

- The table values represent the **field- and time-averaged metrics** across 91 test simulations.
- Mean values highlight the overall model's **consistent high accuracy** throughout the simulations.
- **Standard deviations** remain relatively **small**, indicating low variability in performance across different test cases.

Metric	Mean Error		Standard Deviation
MSE ↓	2e-4	1.4% **RMSE**	2e-4
Conservation of Mass ↓	4e-3	0.4%	3e-3
IoU ↑	0.9996	99.96%	0.0005
SSIM ↑	0.998	99.8%	0.002

*Arrows indicate whether a higher or lower value is better for each metric.

Although datasets differ making direct comparison challenging, prior ML-based fluid simulations report RMSE errors over 10% (Fernández-Godino, 2023; Negiar et al., 2023; Chalapathi et al., 2024; Saad et al., 2024), while our model's error is **ten times lower**.

MSE and Conservation of Mass assess prediction magnitude accuracy, while SSIM and IoU evaluate perceptual and structural differences.

CONCLUSION

Conclusion

- **Porous materials** exhibit unique shock responses, and optimizing porosity distributions allows **for precise shock wave control**.
- The 7-field Spatio-Temporal Model (**7STM**) achieves **fast** full simulation predictions in 7 seconds, reducing computational cost two orders of magnitude compared to simulations.
- The 7STM is **lightweight** and can be run on personal computers.
- The model delivers **highly accurate** predictions, with absolute **errors below 1%** and **perceptual accuracy above 0.99**, maintaining this performance even at late simulation times.
- The fast **shape optimization** enabled by **7STM allows** for a more comprehensive exploration and exploitation of optimal porosity configurations, **advancing the study of shock compression in porous media**.

7STM's **speed, accuracy, and portability** enable rapid and comprehensive optimization, unlocking new opportunities for **discovering enhanced optimal porosity configurations**.

Work in Progress

- Integrate **adjoint information** into the 7STM to enhance gradient-based optimization and improve accuracy in predicting optimal porosity distributions.

- Apply 7STM to real-world experiments for **validation** and further refinement of the predictive framework.

- Integrate 7STM into an **LLM-driven agentic framework** to create an interactive, conversational interface between users and predictive science.

Our team is advancing **exascale optimization** by leveraging deep learning and **LLMs** to expand access to predictive science, accelerate workflows, and **enhance design optimization**.

References

References

1. Chalapathi, N., Du, Y., & Krishnapriyan, A. (2024). Scaling physics-informed hard constraints with mixture-of-experts. ICLR 2024
2. Fernández-Godino, M. G., Chung, W. T., Gowardhan, A. A., Ihme, M., Kong, Q., Lucas, D. D., & Myers, S. C. (2024). A Staged Deep Learning Approach to Spatial Refinement in 3D Temporal Atmospheric Transport. arXiv preprint arXiv:2412.10945.
3. Fernández-Godino, M. G., Lucas, D. D., & Kong, Q. (2023). Predicting wind-driven spatial deposition through simulated color images using deep autoencoders. Scientific Reports, 13(1), 1394.
4. Huy Pham, C., Lorenzana, H. E., Belof, J. L., & Goldman, N. (2023). Hugoniot properties of porous stainless steel: Insights from molecular dynamics simulations. Journal of Applied Physics, 134(4).
5. Jones, K., Lane, J. M. D., & Vogler, T. J. (2018, July). Molecular dynamics study of shock compression in porous silica glass. In AIP Conference Proceedings (Vol. 1979, No. 1). AIP Publishing.
6. Négiar, G., Mahoney, M. W., & Krishnapriyan, A. S. (2023). Learning differentiable solvers for systems with hard constraints. ICLR 2023.
7. R. F. Trunin, L. F. Gudarenko, M. V. Zhernokletov, and G. V. Simakov, Experimental data on shock compression and adiabatic expansion of condensed matter (RFNC-VNIIEF, 2001), pp. 240–251.
8. Saad, F., Burnim, J., Carroll, C., Patton, B., Köster, U., A. Saurous, R., & Hoffman, M. (2024). Scalable spatiotemporal prediction with Bayesian neural fields. Nature Communications, 15(1), 7942.

THANK YOU!

fernandez48@llnl.gov

Presentation available here

Back Up Slides

7STM Architecture